Effect of plasma waves on the optical properties of metal-insulator superlattices

W. Luis Mochán and Marcelo del Castillo—Mussot,
Instituto de Física, Universidad Nacional Autónoma de México,
Apartado Postal 20-364, 01 000 México, Distrito Federal, Mexico

Rubén G. Barrera*
Departamento de Física, Centro de Investigación y de Estudios Avanzados del Instituto Politécnico Nacional,
07000 México, Distrito Federal, México.

(Received 9 June 1986; revised manuscript received 1 October 1986)

We develop a simple transfer-matrix formalism in order to obtain the dispersion relation of the electromagnetic normal modes of an infinite insulator-metal (or highly doped semiconductor) superlattice, taking into account the presence of plasma waves, spatial dispersion, and retardation. We also calculate the p-polarized reflectance and give analytical expressions for the surface impedance, reflection amplitude, and the dispersion relation of the surface modes of a semi-infinite superlattice. We find resonant features corresponding to the propagation of guided plasma waves in the metal layers coupled by transverse fields in the insulating layers. This coupling also yields new bulk modes in regions where propagation would not be allowed without spatial dispersion.

I. INTRODUCTION

When p-polarized light is incident on a conductor, the component of the electric field normal to its surface pushes the conduction electrons towards or away from the surface, creating an excess of charge. If the frequency ω is greater than the plasma frequency ω_p of the conductor, this density fluctuation may propagate as a longitudinal wave, taking along energy from the incident wave. Thus, p-polarized light may couple to bulk plasmons at interfaces, modifying the reflectance away from its Fresnel value.[1] Although the effect of plasma waves on the optical properties of a semi-infinite conductor is usually small,[2] it is resonantly enhanced in thin films near frequencies at which the film thickness is a half integer multiple of the plasmon wavelength. This resonant coupling with guided plasma waves in thin films was first predicted by Farrell[3] and Stern,[4] and was first observed by Lindau and Nilsson[5] and by Anderegg *et al.*[6] The importance of nonlocality or spatial dispersion for the correct understanding of this coupling was first pointed out by Melnyk and Harrison.[2,7] Numerous studies of this effect have been performed using hydrodynamic,[8–10] semiclassical,[11] and microscopic many-body theories.[12–14]

Since the coupling of longitudinal and transverse waves is an interface effect, it may be further enhanced in superlattices in which the interfacial area is proportional to the volume.[15] Technological advances in epitaxial growth have permitted the synthesis of high-quality heterostructures made up of alternating thin layers of lattice matched semiconductors, a few nanometers thick. Their novel electronic properties have been the subject of extensive studies.[16]

The alternating layers of a superlattice originate a periodic modulation of the crystalline potential, which constrains the electronic motion in one direction and originates a series of two-dimensional (2D) bands. By populating only the first 2D band, a quasi-two-dimensional electron gas is produced near each potential minimum. This gas behaves as a 2D conductor since the electrons can move freely along a plane, but a finite amount of energy is required for them to oscillate along the superlattice.[17] Similar results hold for holes.

The collective modes of an isolated, as well as those of infinite and semi-infinite, periodic array of a quasi-2D electron gas, have been studied recently using hydrodynamic[18] and many-body theories.[17,19,20] The results show that each 2D conductor can sustain a 2D plasmon which propagates parallel to the interfaces with wave vector Q and frequency $\omega \propto \sqrt{Q}$. Its electric field extends beyond the electron gas, coupling the 2D plasmons of different layers and giving rise to bulk and surface plasmons for the infinite and semi-infinite superlattice. Its dispersion relation changes from 2D-like to 3D-like as the strength of the coupling is increased.

Qualitatively different systems, not as extensively studied, are obtained by increasing the density of carriers, either by heavy doping[21,22] of a semiconducting superlattice or by fabricating a metallic superlattice.[23] Then, either one or both kinds of layers comprising the heterostructure may behave as a 3D conductor. The normal modes of these systems have a rich structure and they include the following: (i) surface plasmons propagating on each interface and coupled among themselves by the tails of their evanescent fields, giving rise to Bloch waves, (ii) guided, internally reflected, transverse waves in the more dense layers coupled by the evanescent field in the less dense layers, (iii) extended transverse waves in both kinds of layers coupled at their interfaces, (iv) guided plasmon waves in metallic layers coupled by evanescent or propagating transverse waves in dielectric layers, etc.

The first modes mentioned above and their interaction with external probes such as Raman scattering[24] have been studied in the nonretarded limit for finite,[25] infinite,

and semi-infinite superlattices.[26–28] The propagation of transverse waves in multifilm systems is well understood and is of importance in the design of dielectric mirrors, interferometers, and antireflection coatings for optical elements.[1]

Very recently Eliasson *et al.*[21] have studied the modes arising from the coupling of guided and evanescent plasmons in a spatially dispersive metal-metal superlattice ignoring retardation. The effects of spatial dispersion have also been considered by Agranovich and Kravstov,[15] who obtained expressions, within an effective-medium approximation, for the macroscopic dielectric tensor of a superlattice made of very thin layers of excitonic semiconductors. However, to our knowledge, the modes arising from the coupling between plasmons and transverse electromagnetic waves in superlattices have not been investigated previously.

The purpose of this paper is the study of the electromagnetic modes and the optical properties of metal- (or heavily doped semiconductor) insulator superlattices, taking into account retardation, the spatial dispersion of the metallic layers, the propagation of bulk plasmons, and their coupling with transverse waves at the interfaces. We use a novel approach to the problem, consisting of the construction of a 2×2 transfer matrix which relates the electromagnetic field at one interface to the field in the next equivalent interface. This transfer matrix differs from the standard transfer matrices appearing in multifilm optics in that it accounts for the plasma waves inside the metal. The dispersion relation of the bulk and surface modes of the superlattice, as well as its optical properties such as reflectance, are all written simply in terms of the elements of the transfer matrix without any need for further calculations. Since in this paper we concentrate our attention on the propagation of plasmons and their coupling to transverse waves at metallic surfaces, we use a simple hydrodynamic model and a particular additional boundary condition (ABC) of nonelectromagnetic origin. Therefore we ignore several surface-related phenomena[29] which might also be enhanced in superlattices and which should be considered in more realistic calculations. The results of the present paper can be considered the zeroth-order term of a perturbative calculation, where the perturbation parameter is the size of the small surface region where our description of the fields is not accurate.[30]

The present paper is organized as follows. In Sec. II we construct the transfer matrix and we show how to obtain from it the bulk and surface modes and the optical properties of the superlattice. In Sec. III we study our results in different limiting situations, and we compare them to those of local theories and of effective-medium theory. The results of calculations for a model superlattice are presented in Sec. IV, and Sec. V is devoted to our conclusions.

II. THEORY

Let us consider the superlattice, shown in Fig. 1, consisting of alternating insulating and metallic layers of widths a and b, respectively, stacked along the Z direction, on which p-polarized and longitudinal waves propagate. All waves have the same frequency ω, and their wave vectors lie on the XZ plane with a common X component Q. We will construct the transfer matrix of the superlattice by steps: first we will obtain the transfer matrix of the insulator, then the transfer matrix of the metal, and finally we will join them making use of appropriate boundary conditions. We do not consider s-polarized waves since they do not couple to plasmons.

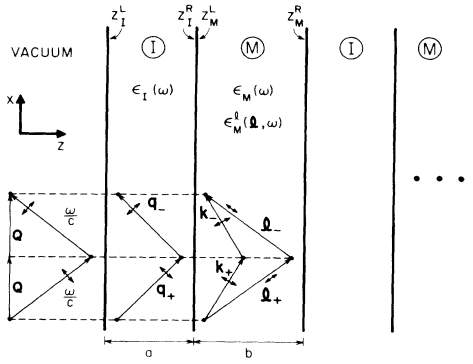

FIG. 1. Metal-insulator superlattice. The wave vectors of the transverse and longitudinal waves and their projection onto the interface planes are shown, together with those of the incident and the reflected light. The coordinate system used and the positions of the left and the right boundaries of a dielectric and a metallic layer are indicated.

A. Insulator

Although the transfer matrix of an insulator is well known, we will show how to construct it in this section in order to introduce our notation and to show a simple procedure which will be generalized in the next section, where we obtain the transfer matrix of a metal.

Given ω and Q, and since we are not considering s-polarized light, there are only two p-polarized waves propagating in the insulator towards the right and left with wave vector $\mathbf{q}_\pm=(Q,0,\pm q)$; the z component $\pm q$ of the wave vector is determined by the wave equation

$$q^2=\epsilon_I\frac{\omega^2}{c^2}-Q^2\ , \tag{1}$$

where c is the speed of light in vacuum and ϵ_I is the insulator's local dielectric function, whose dependence on ω is left implicit. Then, the electromagnetic field anywhere inside a dielectric layer is determined by any two independent field components at one point, such as $E_x(z)$ and $B_y(z)$, the components of the electric and magnetic field parallel to the interface. These are in turn related to the right and left moving contributions to the magnetic field, $B_+(z)$ and $B_-(z)$, through

$$\begin{bmatrix}E_x\\B_y\end{bmatrix}_z=\underline{A}\begin{bmatrix}B_+\\B_-\end{bmatrix}_z\ , \tag{2}$$

where

$$\underline{A}=\begin{bmatrix} Z_I & -Z_I \\ 1 & 1 \end{bmatrix}, \tag{3}$$

and

$$Z_I=\frac{qc}{\epsilon_I\omega} \tag{4}$$

is the surface impedance of the insulator. Here, we have left implicit the dependence $e^{i(Qx-\omega t)}$ of all field quantities.

Since $B_+(z)$ and $B_-(z)$ are plane waves propagating with wave vectors q and $-q$, respectively, they are related at different points z and z' inside the insulator through

$$\begin{bmatrix} B_+ \\ B_- \end{bmatrix}_z=\underline{T}_I(z-z')\begin{bmatrix} B_+ \\ B_- \end{bmatrix}_{z'}, \tag{5}$$

where

$$\underline{T}_I(z-z')=\mathrm{diag}(e^{iq(z-z')}, e^{-iq(z-z')}), \tag{6}$$

and diag$(\cdots)$ denotes a diagonal matrix constructed from the arguments $(\cdots)$. Finally, from (2) and (5) we immediately obtain the transfer matrix

$$\underline{M}_I=\underline{A}\underline{T}_I(a)\underline{A}^{-1}=\begin{bmatrix} \cos(qa) & iZ_I\sin(qa) \\ iY_I\sin(qa) & \cos(qa) \end{bmatrix}, \tag{7}$$

which relates the electromagnetic field at z_I^R, the right boundary of the insulator, to the field at z_I^L, its left boundary (see Fig. 1), through

$$\begin{bmatrix} E_x \\ B_y \end{bmatrix}_{z_I^R}=\underline{M}_I\begin{bmatrix} E_x \\ B_y \end{bmatrix}_{z_I^L}, \tag{8}$$

where $a=z_I^R-z_I^L$ is the insulator's width and $Y_I=1/Z_I$ its surface admittance.

B. Metal

The transfer matrix of the metal layers is obtained following the steps of the preceding section. However, besides a right and a left moving p-polarized wave with wave vectors $\mathbf{K}_\pm=(Q,0,\pm k)$ obeying

$$k^2=\epsilon_M(\omega)\frac{\omega^2}{c^2}-Q^2, \tag{9}$$

we include a right and a left moving longitudinal wave with wave vector $\boldsymbol{l}_\pm=(Q,0,\pm l)$ obeying

$$\epsilon_M^l(\boldsymbol{l}_\pm,\omega)=0, \tag{10}$$

where ϵ_M is the transverse and ϵ_M^l the longitudinal dielectric function of the metal. It is assumed that anywhere inside the metals the field is given by a superposition of these four waves, that ϵ_M is a local response depending only on ω, and that ϵ_M^l is a nonlocal response which is function of l^2 having only one zero for each ω. These assumptions are known as the plasmon pole approximation, which does not yield a very accurate description of the fields near metallic surfaces since it neglects several surface-related effects such as electron-hole pair excitations.[29] However, this is the most simple model to contain the effects of plasma waves, which constitute the subject of this paper, and it yields analytical results which are useful in order to gain physical insight. Where appropriate, we will point out how we expect our results to be modified by more realistic calculations.

Since there are four waves in the metal, the field anywhere inside the metallic layer is determined by any four independent components at one point, such as $E_x(z)$, $B_y(z)$, $E_z(z)$, and $\phi(z)$, where ϕ is the scalar potential in the Coulomb gauge. These are in turn related to the right and left moving contributions to the magnetic field and to the scalar potential $B_+(z)$, $B_-(z)$, $\phi_+(z)$, and $\phi_-(z)$ through

$$\begin{bmatrix} E_x \\ B_y \\ E_z \\ \phi \end{bmatrix}_z=\underline{G}\begin{bmatrix} B_+ \\ B_- \\ \phi_+ \\ \phi_- \end{bmatrix}_z, \tag{11}$$

where

$$\underline{G}=\begin{bmatrix} Z_M & -Z_M & -iQ & -iQ \\ 1 & 1 & 0 & 0 \\ -W_M & -W_M & -il & il \\ 0 & 0 & 1 & 1 \end{bmatrix}, \tag{12}$$

$$Z_M=\frac{kc}{\epsilon_M\omega} \tag{13}$$

is the surface impedance of the metal in the absence of plasma waves, and

$$W_M=\frac{Qc}{\epsilon_M\omega} \tag{14}$$

is a geometric factor that insures transversality of the electric field in the absence of plasma waves.

Since $B_+(z)$ and $B_-(z)$ are transverse, and $\phi_+(z)$ and $\phi_-(z)$ are longitudinal plane waves propagating with wave vectors k, $-k$, l, and $-l$, respectively, they are related at different positions z and z' inside the metal through

$$\begin{bmatrix} B_+ \\ B_- \\ \phi_+ \\ \phi_- \end{bmatrix}_z=\underline{T}_M(z-z')\begin{bmatrix} B_+ \\ B_- \\ \phi_+ \\ \phi_- \end{bmatrix}_{z'}, \tag{15}$$

where

$$\underline{T}_M(z-z')=\mathrm{diag}(e^{ik(z-z')}, e^{-ik(z-z')}, e^{il(z-z')}, e^{-il(z-z')}). \tag{16}$$

Finally, from (11) and (15) we immediately obtain the 4×4 transfer matrix

$$\underline{M}_M=\underline{G}\underline{T}_M(b)\underline{G}^{-1}, \tag{17}$$

which relates the electromagnetic fields at z_M^R, the right boundary of the metal, to the fields at z_M^L, its left boundary, through

$$\begin{bmatrix} E_x \\ B_y \\ E_z \\ \phi \end{bmatrix}_{z_M^R} = \underline{M}_M \begin{bmatrix} E_x \\ B_y \\ E_z \\ \phi \end{bmatrix}_{z_M^L} , \tag{18}$$

where $b = z_M^R - z_M^L$ is the metal's width. We omit the expressions for the matrix elements of $\underline{M}_M$ since they are cumbersome and they are obtained straightforwardly.

C. Boundary conditions

In order to join the metal's 4×4 transfer matrix with the dielectric's 2×2 transfer matrix, we have to point out that although E_x, B_y, E_z, and ϕ are independent quantities in an infinite metal, this is not the case in a thin metallic film bounded by an insulator. The four fields are linearly dependent since they should obey boundary conditions of nonelectromagnetic origin called additional boundary conditions or ABC's.[31,32] There is still some controversy over which are the "correct" ABC's;[9,33,34] different ABC's correspond to different assumptions about the structure of the nonlocal dielectric response $\epsilon_Q(z,z')$ in real space.[35,36] True microscopic models of $\epsilon_Q(z,z')$ do not suffer from these ambiguities.[13]

Given the Coulomb and statistical repulsion between the conduction electrons in the metal, it is reasonable to demand that there be no singularities in their charge density. This, together with Gauss's law implies that E_z should be continuous at the metal's surface. For simplicity we adopt this ABC and we ignore the discontinuity of E_z due to the accumulation at the surface of bound charges. Notice that in the model calculation of Sec. III there are no bound charges. We will take them into account elsewhere.

Since Ampere's law implies that in the insulator $E_z = -W_I B_y$, where

$$W_I = \frac{Qc}{\epsilon_I \omega} , \tag{19}$$

Eq. (18) can be written as

$$\begin{bmatrix} E_x \\ B_y \\ -W_I B_y \\ \phi \end{bmatrix}_{z_M^R} = \underline{M}_M \begin{bmatrix} E_x \\ B_y \\ -W_I B_y \\ \phi \end{bmatrix}_{z_M^L} , \tag{20}$$

where we have also used the continuity of B_y.

Equating the third row with the second row of Eq. (20) multiplied by $-W_I$, a linear relation between ϕ, E_x, and B_y at z_M^L is obtained. Solving the resulting equation for $\phi(z_M^L)$ and substituting back in the right-hand side of Eq. (20), its first two rows become a linear relation between E_x and B_y at z_M^R and E_x and B_y at z_M^L. We write this relation as

$$\begin{bmatrix} E_x \\ B_y \end{bmatrix}_{z_M^R} = \underline{M}'_M \begin{bmatrix} E_x \\ B_y \end{bmatrix}_{z_M^L} . \tag{21}$$

Thus, we have used one ABC on each boundary of a metallic layer in order to collapse its transfer matrix from a 4×4 to the 2×2 matrix M'_M.

The details of the procedure above depend on the particular ABC chosen, although the reduction of the transfer matrix's rank can be performed for any choice of ABC, as long as the layer is bounded by non-spatially-dispersive media. By employing appropriate ABC's our calculations can be performed for other kinds of spatially dispersive layers, such as excitonic semiconductors.[31,37] We are currently developing an alternative expression for the 2×2 transfer matrix of a metallic film in terms of its even and odd surface impedances that can be used in order to go beyond the plasmon pole approximation, i.e., it can be used in situations where the fields are not simply a superposition of a few plane waves.

The last step in the construction of the transfer matrix $\underline{M}$ for a full superlattice period consists of joining $\underline{M}'_M$ and $\underline{M}_I$ using the electromagnetic boundary conditions, i.e., continuity of E_x and B_y, which lead to the simple product

$$\underline{M} = \underline{M}'_M \underline{M}_I . \tag{22}$$

Here, $\underline{M}$ relates the fields E_x and B_y at $z_M^R + d$, or equivalently $z_I^L + d$, to the fields at z_M^R or z_I^L through

$$\begin{bmatrix} E_x \\ B_y \end{bmatrix}_{z_M^R + d} = \underline{M} \begin{bmatrix} E_x \\ B_y \end{bmatrix}_{z_M^R} , \tag{23}$$

where $d = a + b$ is the superlattice period. A similar matrix that translates the fields one period starting from positions z_M^L or z_I^R is obtained by permuting $\underline{M}_I$ and $\underline{M}'_M$ in Eq. (22).

The final expressions for the elements of the transfer matrix are

$$\begin{aligned} M_{11} &= \cos(qa)[\cos(kb) + \mu\nu/D] - Y_I \gamma \sin(qa) , \\ M_{12} &= iZ_I \sin(qa)[\cos(kb) + \mu\nu/D] + i\gamma \cos(qa) , \\ M_{21} &= iY_M \cos(qa)\sin(kb)(1 + \mu/D) \\ &\quad + iY_I \sin(qa)[\cos(kb) + \mu\nu/D] , \\ M_{22} &= \cos(qa)[\cos(kb) + \mu\nu/D] \\ &\quad - Z_I Y_M \sin(qa)\sin(kb)(1 + \mu/D) , \end{aligned} \tag{24}$$

where

$$\begin{aligned} \mu &\equiv Q(W_I - W_M) Y_M \sin(kb) , \\ \nu &\equiv \cos(kb) - \cos(lb) , \\ \gamma &\equiv Z_M \sin(kb) - Q(W_I - W_M)\left[\frac{\sin(lb)}{l} + \frac{\nu^2}{D}\right] , \\ D &\equiv l \sin(lb) - \mu , \end{aligned} \tag{25}$$

and

$$Y_M \equiv 1/Z_M .$$

D. Normal modes

According to Bloch's theorem, the normal modes of a periodic system can always be obtained in the form of

Bloch waves. For an infinite superlattice, this means that

$$\begin{bmatrix} E_x \\ B_y \end{bmatrix}_{z+d} = e^{ipd} \begin{bmatrix} E_x \\ B_y \end{bmatrix}_z , \tag{26}$$

where p is the 1D Bloch's wave vector. Substituting Eq. (26) in Eq. (23) we find that these modes can only exist when $\underline{M} - \underline{1}e^{ipd}$ is a singular matrix, i.e., when

$$\det(\underline{M} - \underline{1}e^{ipd}) = 0 , \tag{27}$$

where $\underline{1}$ is the unit 2×2 matrix.

Since $\det(\underline{M}) = 1$, Eq. (26) can be written simply as

$$\cos(pd) = \tfrac{1}{2}(M_{11} + M_{22}) , \tag{28}$$

or, substituting Eqs. (24) and (25), as

$$\begin{aligned} \cos pd = \Big\{ & \cos(qa)[l \sin(lb)\cos(kb) - Q(W_I - W_M)Y_M \cos(lb)\sin(kb)] \\ & + \sin(qa)\Big[Q(W_I - W_M)Y_I[1 - \cos(lb)\cos(kb)] \\ & - \frac{1}{2}\left[lY_I Z_M + lZ_I Y_M + \frac{Y_I Y_M}{l} Q^2 (W_I - W_M)^2 \right] \sin(lb)\sin(kb) \Big] \Big\} \\ & \times [l \sin(lb) - Q(W_I - W_M)Y_M \sin(kb)]^{-1} , \end{aligned} \tag{29}$$

an expression from which p can be obtained analytically. Notice that if p is a solution of Eq. (29), then $p + 2\pi n$ and $-p + 2\pi n$ are also solutions for any integer n.

E. Optical properties

We now turn our attention to the problem of the reflection of light from a semi-infinite superlattice occupying the $z > 0$ half-space (see Fig. 1). The reflection amplitude is easily calculated once we obtain the surface impedance $Z \equiv (E_x / B_y)_0$ of the superlattice. This in turn can be obtained from the eigenvector equation

$$(\underline{M} - \underline{1}e^{ipd}) \begin{bmatrix} E_x \\ B_y \end{bmatrix}_0 = 0 , \tag{30}$$

and it is given by

$$Z = -\frac{M_{12}}{M_{11} - e^{ipd}} = -\frac{M_{22} - e^{ipd}}{M_{21}} , \tag{31}$$

where, using Eq. (28),

$$e^{ipd} = \tfrac{1}{2}(M_{11} + M_{22}) \pm [\tfrac{1}{4}(M_{11} + M_{22})^2 - 1]^{1/2} . \tag{32}$$

Since the transmitted Bloch wave decays away from the surface or else it propagates towards the right, the correct sign in Eq. (32) is that which makes $|e^{ipd}| < 1$ or, if $|e^{ipd}| = 1$, that which makes $\mathrm{Im}(e^{ipd}) > 0$.

The reflection amplitude is given in terms of the surface impedance by

$$r = \frac{Z_v - Z}{Z_v + Z} , \tag{33}$$

where

$$Z_v = \left[1 - \frac{Q^2 c^2}{\omega^2} \right]^{1/2} = \cos\theta \tag{34}$$

is the surface impedance of vacuum and θ is the angle of incidence. The reflectance R is simply

$$R = |r|^2 . \tag{35}$$

Finally, the surface electromagnetic modes of the semi-infinite superlattice are given by the poles of the reflection amplitude,[30,38] so their dispersion relation is given implicitly by

$$Z_v = -Z . \tag{36}$$

III. LIMITING EXPRESSIONS

In this section we explore the expressions derived above in various limiting situations, and we compare the results obtained with those of previous workers. The local limit corresponds to the case where the charge density is unable to propagate through the metallic layers and is confined in a region of infinitesimal width around the metal-insulator interfaces. This does not mean that longitudinal waves are absent in the metal, but rather, that their decay distance is infinitely small, and therefore the imaginary part of their wave vector is infinitely big. Taking the limit $\mathrm{Im}(l) \to \infty$ in Eqs. (24) we obtain the local transfer matrix:

$$\begin{aligned} M_{11} &= \cos(qa)\cos(kb) - Y_I Z_M \sin(qa)\sin(kb) , \\ M_{12} &= iZ_I \sin(qa)\cos(kb) + iZ_M \cos(qa)\sin(kb) , \\ M_{21} &= iY_I \sin(qa)\cos(kb) + iY_M \cos(qa)\sin(kb) , \\ M_{22} &= \cos(qa)\cos(kb) - Z_I Y_M \sin(qa)\sin(kb) . \end{aligned} \tag{37}$$

Other equations such as Eqs. (28), (31), (33), and (36) remain valid in terms of the local transfer matrix. For example, the dispersion relation of the bulk normal modes (29) becomes

$$\cos(pd)=\cos(qa)\cos(kb) - \frac{1}{2}\left[\frac{\epsilon_M q}{\epsilon_I k}+\frac{\epsilon_I k}{\epsilon_M q}\right]\sin(qa)\sin(kb) . \quad (38)$$

The nonretarded limit of the local dispersion relation is obtained by taking the limit $c\to\infty$, which leads to the equality $q=k=iQ$ according to Eqs. (1) and (9), which substituted in Eq. (38), yield the local nonretarded dispersion relation

$$\cos(pd)=\cosh(Qa)\cosh(Qb) + \frac{1}{2}\left[\frac{\epsilon_M}{\epsilon_I}+\frac{\epsilon_I}{\epsilon_M}\right]\sinh(Qa)\sinh(Qb) . \quad (39)$$

The normal modes obtained from the relations (38) and (39) have been recently studied in Refs. 26, 27, and 28. They correspond to surface plasmons in each interface, coupled to each other by the tail of their evanescent fields, giving rise to a bulk plasma mode.

If the period of the superlattice is much smaller than all the relevant wavelengths, then pd, qa, and $kb \ll 1$ and a second-order expansion of Eq. (38) in these small quantities yields

$$p^2d^2=\frac{\omega^2}{c^2}(\epsilon_I a+\epsilon_M b)d-Q^2(\epsilon_I a+\epsilon_M b)\left[\frac{a}{\epsilon_I}+\frac{b}{\epsilon_M}\right] . \quad (40)$$

This relation is equivalent to Fresnel's dispersion relation for a uniaxial crystal,[39]

$$p^2=\frac{\omega^2}{c^2}\epsilon_x^{\rm ef}-Q^2\epsilon_x^{\rm ef}/\epsilon_z^{\rm ef} , \quad (41)$$

where the dielectric tensor $\overleftrightarrow{\epsilon}^{\rm ef}$ is given by effective-medium theory; since Maxwell's equations imply that E_x and D_z are slowly varying functions of z, then

$$\epsilon_x^{\rm ef}=(\epsilon_I a+\epsilon_M b)/d$$

and (42)

$$(\epsilon_z^{\rm ef})^{-1}=(\epsilon_I^{-1}a+\epsilon_M^{-1}b)/d .$$

In this limit the reflection amplitude is given simply by

$$r=\frac{\epsilon_x^{\rm ef}\cos\theta-pc/\omega}{\epsilon_x^{\rm ef}\cos\theta+pc/\omega} , \quad (43)$$

and the surface electromagnetic modes by

$$Q^2=\frac{(\epsilon_x^{\rm ef}-1)\epsilon_z^{\rm ef}}{\epsilon_x^{\rm ef}\epsilon_z^{\rm ef}-1}\frac{\omega^2}{c^2} . \quad (44)$$

Finally, we obtain the dispersion relation of the normal modes of the superlattice in the long-wavelength approximation, but taking now into account the propagation of longitudinal waves. This is done by expanding Eq. (29) up to second order in pd, qa, and kb, leading to

$$l\sin(lb)\left[\left[p^2-\frac{\omega^2}{c^2}\epsilon_x^{\rm ef}+Q^2\frac{\epsilon_x^{\rm ef}}{\epsilon_z^{\rm ef}}\right]d^2-\frac{(\epsilon_M-\epsilon_I)^2}{\epsilon_M\epsilon_I}\frac{Q^4}{l^2}ab\right]+2[1-\cos(lb)]\left[\frac{1}{\epsilon_I}-\frac{1}{\epsilon_M}\right]\epsilon_x^{\rm ef}Q^2d=0 . \quad (45)$$

We did not attempt a power expansion in lb since longitudinal waves typically have a much smaller wavelength than transverse waves, except for a very short frequency range around ω_p.

Several properties of the electromagnetic normal modes of the superlattice can be obtained from a simple analysis of the dispersion relation (45). First, we remark that for propagation along the superlattice ($Q=0$), the normal modes are either transverse waves propagating with the speed $c/(\epsilon_x^{\rm ef})^{1/2}$ or standing plasma oscillations in each metallic layer with frequencies ω_n such that $l=n\pi/b$, where n is an integer. Since each metallic region is isolated from the others by dielectric layers, their corresponding plasmons do not interact between themselves and so the frequency of the longitudinal modes is independent of the wave vector p, their group velocity is zero, and therefore they cannot transport energy.

Notice that even if $Q\neq 0$, the even-numbered standing plasmons whose wavelength fits an integer number of times in the metal's width b do not propagate (in the long-wavelength approximation), since they solve Eq. (45) for any value of p. The reason for this is that in each metal they have an equal amount of positive and negative charge at each x, i.e.,

$$\int_{z_M^L}^{z_M^R} dz\,\rho(x,z)=0 ,$$

where $\rho(x,z)$ is the volume charge density. Therefore, the electric field produced by the charge distribution is very small outside of the metallic layers, leading to a negligible interaction. This cancellation does not occur for the odd-numbered standing plasmons, whose wavelength fits a half-integer number of times. From Eq. (45) these modes correspond to poles of the wave vector $p(\omega)$.

For frequencies $\omega>\omega_p$, $\omega\neq\omega_n$, the modes are a mixture of transverse and longitudinal waves, and p oscillates around its local value given by Eq. (41). Finally, if $\omega<\omega_p$, the longitudinal wave vector l becomes imaginary and large and the local approximation becomes appropriate.

IV. MODEL CALCULATION

In this section we present the results of analytical calculations performed for a model superlattice, in which the conducting layers have a Drude transverse dielectric function

$$\epsilon_M(\omega)=1-\frac{\omega_p^2}{\omega^2+i\omega/\tau}\ , \tag{46}$$

and a hydrodynamic longitudinal response

$$\epsilon_M^l(l,\omega)=1-\frac{\omega_p^2}{\omega^2+i\omega/\tau-\beta^2(Q^2+l^2)}\ , \tag{47}$$

where τ is the electronic relaxation time and $\beta^2=3v_F^2/5$, with v_F the Fermi velocity of the metal. The factor of $\frac{3}{5}$ is obtained from a long-wavelength expansion of Lindhard's dielectric response.[40] We chose vacuum as an insulator so that $\epsilon_I=1$, and we took $\tau=100/\omega_p$ and $v_F=0.01c$.

In Fig. 2 we show the dispersion relation for a superlattice with $a=b=0.1\lambda_p$ and a fixed value of $Q=1.5/\lambda_p$, where $\lambda_p\equiv c/\omega_p$. In order to obtain Fig. 2 we gave real values to ω and then solved Eq. (29) analytically for the real and the imaginary part of the Bloch's wave vector p; the solid line corresponds to the solution with a positive imaginary part while the dashed-dotted line corresponds to the solution with a negative imaginary part. Notice that for some frequencies it is not possible to have both a positive imaginary part and a positive real part in the first Brillouin zone. Thus, Bloch waves which decay towards the right may seem to propagate towards the left.

In order to understand the main features of Fig. 2, it is useful to compare it with Fig. 3, where we plotted the dispersion relation for the same system but in the local limit. This was obtained from Eq. (38) although it is almost indistinguishable from the effective-medium result given by Eq. (40) since we chose such small values for a and b. We also plotted in Fig. 3 the dispersion relation of the longitudinal waves $\omega=\omega_n$ assuming they do not interact with transverse waves at the conductor surfaces and assuming an infinite relaxation time τ, since they cannot exist with real frequencies if τ is finite.

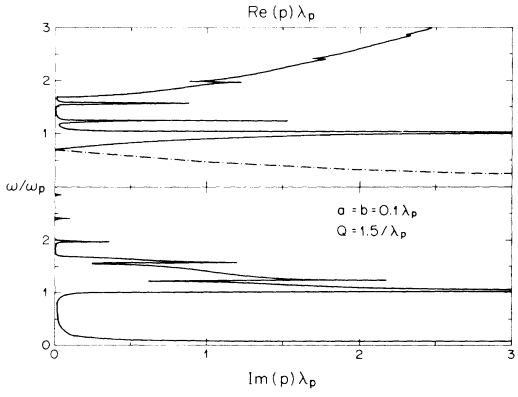

FIG. 2. Dispersion relation ω vs p of a superlattice with $a=b=0.1\lambda_p$ and with $Q=1.5/\lambda_p$. The real part of p is shown in the upper panel and its imaginary part in the lower panel. The solid line corresponds to the branch with a positive imaginary part and the dashed-dotted line to the branch with a negative imaginary part.

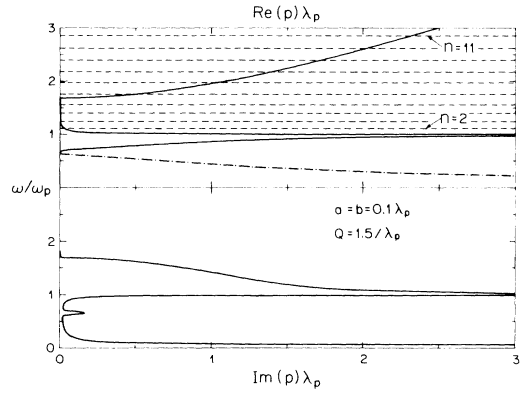

FIG. 3. Dispersion relation ω vs p of a superlattice with $a=b=0.1\lambda_p$ and $Q=1.5/\lambda_p$, in the local limit. Also shown with dashed lines is the dispersion relation of guided plasma waves in the absence of damping and of longitudinal-transverse interaction.

At frequencies near the surface plasma frequency of an isolated metal-vacuum interface, $\omega_s=\omega_p/\sqrt{2}$, two propagating normal modes can be seen: one whose frequency diminishes and another whose frequency increases with increasing wave vector p. Since these modes have $\omega<\omega_p<Qc$, they are made up of evanescent waves in both the conducting and the insulating layers, i.e., q and k are almost imaginary. Actually, they consist of surface plasmons localized on each interface but interacting among themselves through the tails of their evanescent fields, thus giving rise to bulk modes of the whole superlattice. Recall that for an isolated thin metallic film there are two surface plasmons: a symmetric one with equal charges and an antisymmetric one with opposite charges on the two surfaces of the film, the former having a smaller frequency than the latter. When many metallic films are brought near each other to form a superlattice, each of these two kinds of surface plasmons gives rise to a bulk band. These two bands have been studied recently in Refs. 26 and 27 within the nonretarded limit.

The behavior of the coupled surface plasmon bands can be discussed qualitatively by referring to Fig. 4, where we show two of the metallic layers comprising the superlattice and the sign of the charges induced at their surfaces. We also show with arrows the attraction or repulsion between the electrons on a selected surface and the charges on neighboring surfaces. Figure 4(a) shows symmetric surface plasmons which alternate sign between adjacent conductors and therefore have $p=\pi/d$. It can be seen that the repulsion of the electrons on the same conductor and the attraction to the positive charges in the neighboring conductor press the selected electrons onto the surface, impeding their motion in the Z direction and leading to a small frequency of oscillation. As p diminishes towards zero we approach the situation illustrated in Fig. 4(b), where charges in the same and in different layers push in opposite directions therefore subtracting their effects and leading to a higher frequency. Figure 4(c) corresponds to

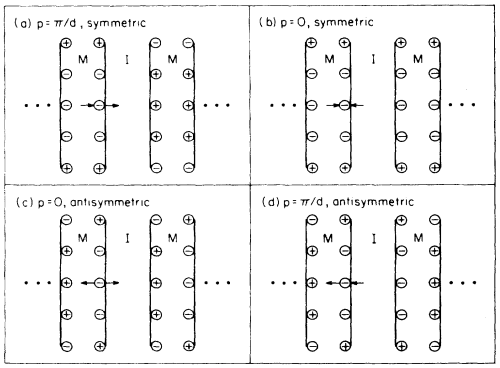

FIG. 4. Surface charge configurations in coupled surface plasmon bands: (a) symmetric surface plasmon on each metallic layer alternating sign between layers, (b) symmetric surface plasmons with the same phase on each metallic layer, (c) antisymmetric surface plasmons with the same phase, and (d) antisymmetric surface plasmons alternating sign. The direction of the forces "felt" by the electrons in one surface due to the charges on the opposite surface of the same layer and on the facing surface of the following layer are indicated.

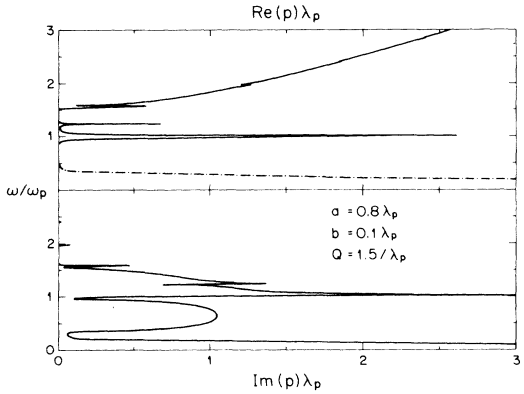

FIG. 5. Dispersion relation ω vs p of a superlattice with $a=0.8\lambda_p$, $b=0.1\lambda_p$, and $Q=1.5/\lambda_p$.

antisymmetric surface plasmons oscillating in phase. In this case, charges in the same and in different layers pull in opposite directions giving rise to a situation similar to that of Fig. 4(b). Finally, as the phase difference between adjacent layers increases, we approach Fig. 4(d) where $p=\pi/d$. Here, the attraction to the positive charges in the same layer and the repulsion of the charges in the facing surface drive the electrons away from the surface, leading to a high oscillation frequency. Thus, the situation in Fig. 4(a) has the lowest and that of Fig. 4(d) the highest frequency; the relative frequencies of the oscillations shown in Fig. 4(b) and 4(c) depend on the widths of the metallic and the insulating layers.

In the nonretarded region, the surface plasmon fields decay as we move away from the surface, either into the metal or into the dielectric, with the same decay length $1/Q$. Therefore, if $a=b$, the opposing forces shown in Figs. 4(b) and 4(c) cancel each other exactly and the surface plasmon on any given surface is undisturbed by the presence of the other surfaces of the superlattice. Thus the oscillations in Figs. 4(b) and 4(c) become degenerate and they have the frequency $\omega=\omega_s$ of the surface plasmon of a semi-infinite metal. This degeneracy of the two kinds of surface plasmon bands at $p=0$ is broken by retardation, since it makes the decay length in the metal $[1/\mathrm{Im}(k)]$ smaller than that in the dielectric $[1/\mathrm{Im}(q)]$ according to Eqs. (1) and (9), so that the metallic films appear to be thicker.

The degeneracy at $\omega=\omega_s$ can be seen in the upper panel of Fig. 3, where the two surface plasmon bands touch each other at $\mathrm{Re}(p)=0$. The fact that the degeneracy is not exact can be seen in the lower panel as a small peak in $\mathrm{Im}(p)$ at $\omega=\omega_s$. Actually, in the nondissipative limit, $\tau\to\infty$, a small gap would open at $\mathrm{Re}(p)=0$. On the other hand, the charges shown at the metals' surfaces in Fig. 4 occupy a region with a nonzero width $1/\mathrm{Im}(l)$, so that, when spatial dispersion is taken into account, the metallic films appear to be thinner. In Fig. 2 we took into account both retardation and spatial dispersion. Since their effects compete with each other, the two surface plasmon bands appear to be degenerate at $\mathrm{Re}(p)=0$ and there is no longer a peak in $\mathrm{Im}(p)$ near $\omega=\omega_s$. Another effect of spatial dispersion on the surface plasmon bands is a slight increase in their frequency. In more elaborate models, such as the random-phase-approximation (RPA) self-consistent jellium, we expect another competing effect: a nonvanishing conduction electron density outside the metal layers. This electron spillout would tend to make the metallic films appear thicker and to decrease their surface plasmon frequency.[29]

Going up in frequency, it can be seen that the dispersion relations shown in Figs. 2 and 3 are very similar to each other except for a series of peaks in the nonlocal calculation at the frequencies $\omega=\omega_n$ for odd values of n. Notice that there are no visible effects of the longitudinal

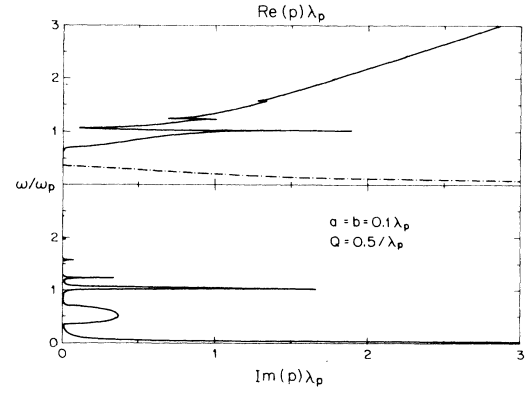

FIG. 6. Dispersion relation ω vs p of a superlattice with $a=b=0.1\lambda_p$ and $Q=0.5/\lambda_p$.

waves for even values of n, as was discussed in the preceding section.

Between $\omega=\omega_p$ and $\omega=1.7\omega_p$ there can be no propagation according to the local dispersion relation, i.e., $\mathrm{Re}(p)\approx 0$ and $\mathrm{Im}(p)$ is large in Fig. 3. However, two propagating modes can be seen inside this gap in Fig. 2 at $\omega=\omega_3$ and ω_5. In the former, $\omega<Qc<(\omega_p^2+Q^2c^2)^{1/2}$ and therefore transverse waves cannot propagate in vacuum nor in the metal according to Eqs. (1), (9), and (46). Thus, the mode at $\omega=\omega_3$ consists of guided plasma waves propagating inside the metallic films with wave vector Q and being reflected back and forth from the metals' surfaces on which they interact with evanescent transverse waves. The tail of the evanescent fields in vacuum couple the guided plasma waves in neighboring metallic films, giving rise to the bulk mode.

Since $\omega_5>Qc$, the mode at $\omega=\omega_5$ can be thought of as being made up of either guided plasma waves in the metals coupled to each other through extended transverse waves in the dielectrics, or conversely, as extended transverse waves in the dielectrics coupled by the guided plasma waves in the metallic layers.

For $\omega\geq 1.7\omega_p$ propagation of bulk modes becomes possible in the local limit as can be seen in Fig. 3, where $\mathrm{Im}(p)\approx 0$ and $\mathrm{Re}(p)\neq 0$. These modes consist of extended waves in the dielectrics coupled through either extended, for $\omega>(\omega_p^2+Q^2c^2)^{1/2}$, or evanescent waves in the metals. The odd-numbered guided plasma waves at ω_7, ω_9, etc., modify the strength of this coupling giving rise to the small peaks in $\mathrm{Re}(p)$ that can be seen in Fig. 2. They also absorb energy resonantly, originating sharp peaks in $\mathrm{Im}(p)$.

The detailed shape and size of the features found in Fig. 2 at the frequencies ω_3, ω_5, etc., depend on the strength of the coupling between transverse and longitudinal waves at the metal's surface. This is in turn sensitive to the microscopic surface structure, since there is no transverse-longitudinal coupling in the bulk. Thus, in a model such as the RPA self-consistent jellium, in which the electronic density does not fall sharply to zero at the interface and in which excitation of electron hole pairs is possible, this coupling is smaller than in the hydrodynamic model.[29] However, the presence of resonant structure similar to that shown in Fig. 2 is unavoidable in any nonlocal theory.

In Fig. 5 we show the dispersion relation for the same system as that in Fig. 2, except that we made the insulators' width, $a=0.8\lambda_p$, wider than the metals' width, $b=0.1\lambda_p$. As expected from the discussion above, when a and b differ, a gap opens between the upper and the lower surface plasmon bands. Thus, Fig. 5 shows that no propagation is possible between $0.3\omega_p$ and $0.9\omega_p$, where $\mathrm{Re}(p)\approx 0$ and $\mathrm{Im}(p)$ has a large peak. In other respects, Fig. 5 is similar to Fig. 2; the gap above ω_p is somewhat narrower and the effect of the guided plasmon is smaller simply because the corresponding superlattice contains less metal.

The effects of retardation are illustrated in Fig. 6, which corresponds to the same system as in Fig. 2, but now with a smaller wave vector $Q=0.5/\lambda_p$ parallel to the interfaces. As Q diminishes, the frequency of the lower surface plasmon band is pushed down, so that it remains always below the light line $\omega=Qc$. This band starts at $0.33\omega_p$ in Fig. 6. On the other hand, the upper surface plasmon band evolves continuously into the band that starts at ω_s in Fig. 6. However, this can no longer be regarded as a surface plasmon band since it is now above the light line, and therefore the fields in the dielectric layers are no longer evanescent. No propagation is possible in between these two bands. It can also be seen in Fig. 6 that the gap above ω_p practically disappeared since the metal becomes transparent at a smaller frequency $(\omega_p^2+Q^2c^2)^{1/2}$, and that the effect of the guided plasmons decreased, as it should ultimately disappear at $Q=0$.

In order to show the effects of the periodicity of the superlattice, in Fig. 7 we have plotted the dispersion relation for a system with a bigger period, $a=b=\lambda_p$, and for

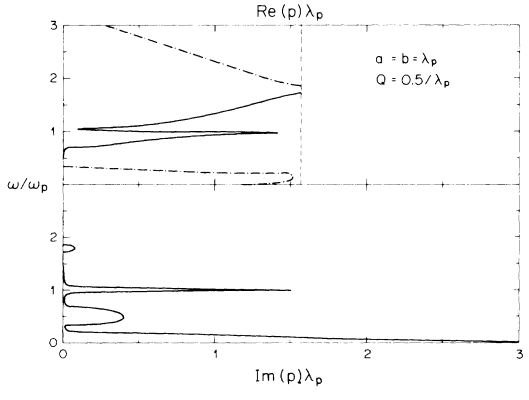

FIG. 7. Dispersion relation ω vs p of a superlattice with $a=b=\lambda_p$ and $Q=0.5/\lambda_p$. The vertical dashed line indicates the boundary of the Brillouin zone.

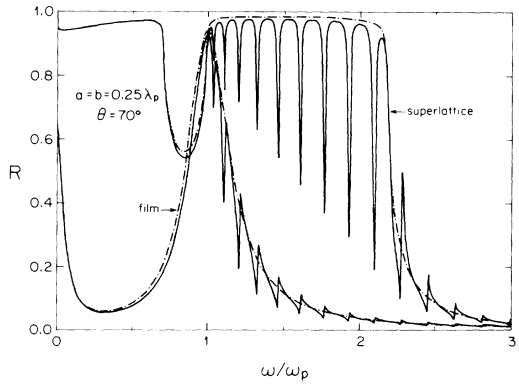

FIG. 8. Nonlocal (solid line) and local (dashed-dotted line) calculation of the reflectance of a semi-infinite superlattice and of a metallic film with $a=b=0.25\lambda_p$ for an angle of incidence $\theta=70°$.

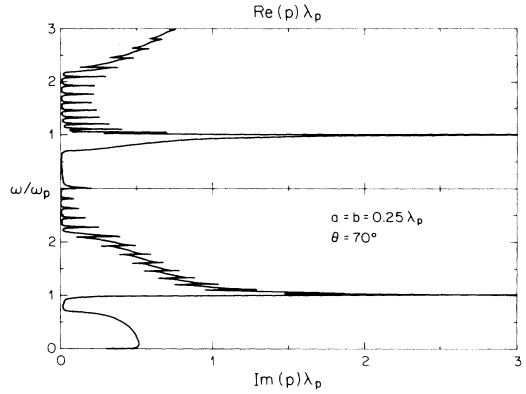

FIG. 9. Dispersion relation ω vs p of a superlattice with $a=b=0.25\lambda_p$ for a fixed angle of incidence $\theta=70°$.

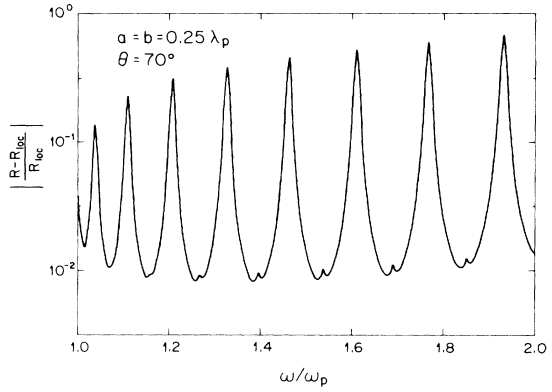

FIG. 10. Normalized difference $|R-R_{\rm loc}|/R_{\rm loc}$ between the nonlocal and the local calculation of the reflectance of a superlattice with $a=b=0.25\lambda_p$ for an angle of incidence $\theta=70°$.

$Q=0.5/\lambda_p$. It can be seen that gaps are opened at the edge of the Brillouin zone corresponding to $\mathrm{Re}(p)=\pi/2\lambda_p$, of which the clearest is the one around $1.75\omega_p$; the one around $0.1\omega_p$ is rounded off by the high dissipation. Since the metals' width b is big, the guided plasmon frequencies ω_n are very close together. However, their decay distance is smaller than b so their small effect on the dispersion relation is not noticeable in the figure.

In Fig. 8 we show the reflectance of a semi-infinite superlattice with $a=b=0.25\lambda_p$ for an angle of incidence of $\theta=70°$. We included results of both nonlocal and local calculations obtained from Eqs. (24), (31)—(35), and (37). In order to understand their features, we have plotted in Fig. 9 the dispersion relation $\omega(p)$ calculated for a fixed angle of incidence instead of for a fixed Q. We see that the reflectance is almost 1 in the regions where there is no propagating normal mode in the superlattice, and it diminishes where propagation is permitted. The nonlocal reflectivity has a series of sharp, deep minima between ω_p and $2.2\omega_p$, corresponding to plasmon-mediated propagation inside the local gap. This structure is less noticeable above $2.2\omega_p$, where propagation is permitted in the local case. As a comparison we have also plotted in Fig. 8 the reflectance of a single metal film; the plasma resonances are clearly visible at the same frequencies but they are much less prominent than in the superlattice. The depth of the reflectance minima due to the plasmon-mediated propagation in the superlattice might be modified in more realistic models of the metals. However, we expect their presence and their big enhancement over the corresponding structures for a single metal film to be independent of the particular nonlocal model employed.

Finally, in Fig. 10 we show a logarithmic plot of $|R-R_{\rm loc}|/R_{\rm loc}$ for the same superlattice as in Fig. 9, where $R_{\rm loc}$ is the reflectance in the local limit. The high peaks correspond to the frequencies of the odd-numbered guided plasma waves. The even-numbered plasmons are responsible for the small peaks seen near the minima. Thus, they do interact with transverse waves although their effect is about three orders of magnitude smaller.

V. CONCLUSIONS

In this paper we developed a novel approach to the calculation of the optical properties of metal-insulator superlattices. The 2×2 electromagnetic transfer matrix of the superlattice was obtained as a product of the transfer matrix of an insulating and a metallic layer. In order to take into account the propagation of plasma waves in the metal, its transfer matrix had to be enlarged to a 4×4 matrix, which was later collapsed to a 2×2 matrix by introducing additional boundary conditions. Simple expressions were then derived for the dispersion relation of the bulk and surface modes of the superlattice, as well as for its reflection amplitude, and they were explored in several limiting cases. Analytical calculations within a simple hydrodynamic model were performed in order to illustrate the effects of retardation, periodicity, and spatial dispersion on the optical properties of the superlattice.

The most important result shown is the existence of propagating bulk modes, made up of coupled guided plasmons, in regions where no propagation is expected if spatial dispersion is neglected. These modes manifest themselves as a series of very sharp and very deep minima in the reflectance of a semi-infinite superlattice near frequencies ω_n for which the wavelength of the plasmons fits a half-integer number of times $n/2$ on the metallic layers' width, where n is an odd integer. These minima are much more pronounced than those found in single metallic films, and they should be easily observable experimentally. Our physical picture is that at these frequencies the plasmons of a given metallic layer interact with the transverse waves on the neighboring dielectric layers, taking energy from the preceding one, partially dissipating it, and partially transporting it across the metal and giving it away to the next dielectric. This plasmon-mediated propagation through the metallic films is impossible without spatial dispersion.

Although we obtained our present results by using a hydrodynamic model and assuming a specific ABC, namely,

continuity of the normal component of the electric field, we do not expect our qualitative results to be modified by a different choice of ABC or by using more realistic models. By an appropriate choice of ABC and of dielectric function they can also be adapted to excitonic semiconductor superlattices. Our formulas can also be used for metal-metal superlattices at frequencies below the plasma frequency of the more dense metal, ignoring the small effects of spatial dispersion in it. At higher frequencies charge fluctuations are able to propagate in both metals and the metal-metal superlattice can no longer be characterized by a 2×2 transfer matrix. However, a 4×4 transfer matrix can be constructed from those of its constituents, and from it, the normal modes and optical properties of the metallic superlattice can be obtained following a procedure analogous to the one shown in this paper. Work in that direction is currently under progress.

ACKNOWLEDGMENTS

We want to thank J. J. Quinn, M. Harrison, W. L. Schaich, and F. Soto for useful discussions. This work was supported in part by Consejo Nacional de Ciencia y Tecnología (México) through Grant No. PCEXNA-040428.

*Permanent address: Instituto de Física, Universidad Nacional Autónoma de México, Apartado Postal 20-364, 01 000 México D.F., México.

[1]M. Born and E. Wolf, *Principles of Optics* (MacMillam, New York, 1964), Chap. I.
[2]R. A. Melnyk and M. J. Harrison, Phys. Rev. B **2**, 835 (1970).
[3]R. A. Farrell, Phys. Rev. **111**, 1214 (1958).
[4]R. A. Farrell and E. A. Stern, Am. J. Phys. **30**, 810 (1962).
[5]I. Lindau and P. O. Nilsson, Phys. Lett. **31A**, 352 (1970); Phys. Scr. **3**, 87 (1971).
[6]M. Anderegg, B. Feurbacher, and B. Fitton, Phys. Rev. Lett. **27**, 1565 (1971).
[7]R. A. Melnyk and M. J. Harrison, Phys. Rev. Lett. **31**, 85 (1968).
[8]A. D. Boardman, B. V. Paranjape, and Y. O. Nakamura, Phys. Status Solidi B **75**, 347 (1976).
[9]F. Forstmann and H. Stenschke, Phys. Rev. Lett. **38**, 1365 (1977); Phys. Rev. B **17**, 1489 (1978).
[10]W. L. Schaich and C. Schwartz, Phys. Rev. B **25**, 7365 (1982); C. Schwartz and W. L. Schaich, J. Phys. C **17**, 537 (1984).
[11]K. L. Kliewer and R. Fuchs, Phys. Rev. **172**, 607 (1968); R. Fuchs and K. L. Kliewer, Phys. Rev. **185**, 905 (1968).
[12]T. Maniv and H. Metiu, Phys. Rev. B **22**, 4731 (1980); J. Chem. Phys. **76**, 2697 (1982).
[13]P. J. Feibelman Phys. Rev. B **23**, 2629 (1969); **12**, 1319 (1975).
[14]P. Garik and N. W. Ashcroft, Solid State Commun. **39**, 1183 (1981).
[15]V. M. Agranovich and V. E. Kravstov, Solid State Commun. **55**, 85 (1985).
[16]L. Esaki, J. Phys. (Paris) Colloq. **45**, C5-3 (1984).
[17]Proceedings of the Fourth International Conference on Electronic Properties of Two-Dimensional Systems, New London, New Hampshire, 1981, edited by F. Stern [Surf. Sci. 113 (1982)].
[18]A. L. Fetter, Ann. Phys. (N.Y.) **81**, 367 (1973); **88**, 1 (1978).
[19]S. Das Sarma and J. J. Quinn, Phys. Rev. B **25**, 7603 (1982).
[20]J. K. Jain and P. B. Allen, Phys. Rev. Lett. **54**, 947 (1985).
[21]G. Eliasson, G. F. Giuliani, and J. J. Quinn, Phys. Rev. B **33**, 1405 (1986).
[22]H. Köstlin, R. Jost, and W. Lems, Phys. Status Solidi A **29**, 87 (1975); I. Hanberg, C. G. Granqvist, K. F. Berggren, B. E. Sernelius, and L. Ergström, Vacuum **35**, 207 (1985); F. Demichelis, E. Minetti-Mezzeti, V. Smurro, A. Tagliaferro, and E. Tresso, J. Phys. D **18**, 1825 (1985).
[23]Z. A. Zheng, C. M. Falco, and J. B. Ketterson, Appl. Phys. Lett. **38**, 424 (1981); I. K. Schiller and C. M. Falco, Surf. Sci. **113**, 443 (1982).
[24]P. Hawrylak, J. W. Wu, and J. J. Quinn, Phys. Rev. B **32**, 5169 (1985).
[25]G. M. Arutyunyan and Kh. V. Nerkarayan, Opt. Spektrosk. **56**, 97 (1984) [Opt. Spectrosc. (USSR) **56**, 60 (1984)]; B. L. Johnson, J. T. Weiler, and R. E. Camley, Phys. Rev. B **32**, 6544 (1986).
[26]R. E. Camley and D. L. Mills, Phys. Rev. B **29**, 1695 (1984).
[27]G. F. Giuliani, J. J. Quinn, and R. F. Walls, J. Phys. (Paris) Colloq. **45**, C5-285 (1984); R. Szenics, R. F. Wallis, G. F. Giuliani, and J. J. Quinn, Surf. Sci. **166**, 45 (1986).
[28]H. Shi and C.-H. Tsai, Solid State Commun. **52**, 953 (1984).
[29]P. J. Feibelman, Prog. Surf. Sci. **12**, 287 (1982).
[30]W. L. Mochán, R. Fuchs, and R. G. Barrera, Phys. Rev. B **27**, 771 (1983).
[31]S. I. Pekar, Zh. Eksp. Teor. Fiz. **33**, 1022 (1957) [Sov. Phys.—JETP **6**, 785 (1958)].
[32]F. Sauter, Z. Phys. **203**, 488 (1967).
[33]F. Forstmann, Z. Phys. **32**, 385 (1979).
[34]P. Ahlqvist and P. Apell, Phys. Scr. **25**, 587 (1982).
[35]D. L. Johnson and P. R. Rimbey, Phys. Rev. B **4**, 2398 (1976).
[36]P. Halevi and G. Hernández-Cocoletzi, Phys. Rev. Lett. **48**, 1500 (1982).
[37]J. J. Hopfield, Phys. Rev. **112**, 1555 (1958); J. J. Hopfield and D. G. Thomas, *ibid.* **122**, 35 (1961); **132**, 563 (1963); G. D. Mahan and J. J. Hopfield, Phys. Rev. A **135**, 428 (1964); J. J. Hopfield, in Proceedings of the Eighth International Conference on the Physics of Semiconductors, Kyoto 1966 [J. Phys. Soc. Jpn. Suppl. **21**, 77 (1966)].
[38]B. B. Dasgupta and A. Bagchi, Phys. Rev. B **19**, 4935 (1979).
[39]L. D. Landau and E. M. Lifshitz, *Electrodynamics of Continuous Media* (Pergamon, New York, 1960) Sec. 77.
[40]J. Lindhard, Kgl. Danske Videnskab. Selskab, Mat.-Fys. Medd. **28**, 8 (1954).